Turk J Chem
31 (2007) , 455 – 464.

Low Temperature CO Oxidation Kinetics over Activated Carbon Supported Pt-SnO_x Catalysts

Fatma Soyal BALTACIOĞLU, Berrin GÜLYÜZ,
Ahmet Erhan AKSOYLU, Zeynep İlsen ÖNSAN*
Department of Chemical Engineering, Boğaziçi University, Bebek 34342, İstanbul-TURKEY
e-mail: onsan@boun.edu.tr

Received 23.03.2007

The kinetics of low temperature CO oxidation were studied over sequentially impregnated 1wt%Pt-0.25wt%SnO_x supported on HNO_3-oxidized activated carbon (AC3) using a wide range of CO (1-10 mol%) and O_2 (1-4 mol%) concentrations. Intrinsic kinetic data were obtained in the initial rates region at 383 K in the absence and presence of 5-45 mol% H_2 in the feed. A power-function rate expression with positive dependence on CO (0.96) and negative dependence on oxygen (–0.31) was obtained for the low temperature oxidation of CO. The effect of H_2 on CO oxidation rates was also investigated under similar conditions.

Key Words: Carbon monoxide, oxidation, kinetics, Pt-Sn catalysts, activated carbon supports, PROX.

Introduction

Proton exchange membrane fuel cells are among the most promising fuel cell technologies for stationary heat and power generation and for automotive applications due to their high power density and relatively low operating temperature. A crucial requirement for PEM fuel cells is the complete removal of the CO in the exit H_2 stream coming from hydrocarbon fuel reforming and water gas shift reactors. An efficient and economical way of producing CO-free hydrogen is to place a preferential CO oxidation (PROX) reactor immediately after the low temperature water-gas-shift converter in order to reduce the CO content from 0.5-1 mol% to 10-50 ppm before the H_2 stream enters the PEM fuel cell. Exit gas temperatures from the low temperature water-gas-shift reactor are in the 473-523 K range and the PEM fuel cell operates at around 353-373 K, which puts the temperature range for low temperature CO oxidation between 373 and 423 K.[1,2]

Supported noble metal catalysts have generally been considered for promoting CO oxidation. These catalysts are not efficient at low temperatures (< 443 K) or low O_2/CO ratios, because CO and O_2 compete for similar sites and strong CO adsorption prevents O_2 adsorption by blanketing the metal surface.[1,3] Among the composite catalysts proposed for low temperature CO oxidation, noble metal reducible oxide (NMRO) combinations are prominent since they give significantly higher catalytic activity by providing suitable sites

*Corresponding author

for both CO and O_2 chemisorption. Pt-based catalysts supported on various materials have been studied in this context.[1,2] It is necessary to evaluate these catalysts first in terms of low-temperature CO oxidation, and then in terms of PROX in the presence of H_2.

One of the composite catalysts initially used for the low temperature oxidation of CO is Pt-SnO_2. A synergistic interaction is indicated by the high activity of Pt-SnO_2 at temperatures well below 150 °C where neither Pt nor SnO_x alone can catalyze CO oxidation.[4] The nature of this interaction and the mechanism of low-temperature CO oxidation over Pt-SnO_2 are still being explored. Reaction rate measurements conducted in the absence of H_2 over γ-Al_2O_3 supported Pt-SnO_2 indicate that the most likely mechanism is the dissociative adsorption of oxygen on reducible SnO_2 sites followed by oxygen reverse-spillover onto the Pt metal and reaction with CO chemisorbed on Pt.[5,6] It is also suggested that oxygen can adsorb on both Pt and SnO_2 sites while CO chemisorption is limited to Pt sites only.[4]

Several Pt-SnO_x catalysts supported on non-oxidized, air-oxidized, and HNO_3-oxidized activated carbons (AC1, AC2, and AC3, respectively) were characterized in detail using N_2 adsorption, TPD, TPR, H_2 adsorption, XPS, SEM-EDX, XRD, and structure-insensitive probe reactions to show that oxidative pretreatments modify the chemical properties of the support surface as well as enhancing Pt dispersion and promoting Pt_3Sn alloy formation.[7] The results of subsequent low-temperature CO oxidation experiments over 1%Pt-0.25%SnO_x/AC catalysts in a H_2-free feed stream clearly showed that the catalyst prepared by sequential impregnation on the AC3 support had the highest activity with 100% CO conversion at 398 K.[8]

When the AC supported catalysts were tested for their low-temperature PROX activity in a H_2-rich stream containing 1 mol% CO, 1 mol%O_2, and 60 mol% H_2, the 1%Pt-0.25%SnO_x/AC2 catalyst gave the highest CO conversion of 81% with a CO oxidation selectivity of 41%, indicating the beneficial effect of the thermally stable oxygen-bearing surface groups of the air-oxidized AC support.[9] Addition of 15 mol% CO_2 to the H_2-rich feed led to drastic increases in the CO conversion levels of 1%Pt-0.25%SnO_x catalysts on oxidized AC supports, which is unlike the CO_2 effect observed on all other selective CO oxidation catalysts prepared with other support materials.[10] Further addition of 10 mol% H_2O to the H_2-rich feed stream containing CO_2 (for simulating the actual composition of the reformate from the water-gas-shift converter) enhanced the activity and selectivity obtained over both AC2 and AC3 supported catalysts, clearly indicating that they can be potential candidates for use as commercial PROX catalysts. The PROX performance of 1%Pt-0.25%SnO_x/AC3 in H_2-rich feed containing CO_2 and H_2O was superior with 100% CO conversion and 50%-51% CO oxidation selectivity at extended times on stream.[10]

The aim of the present work was to evaluate 1wt%Pt-0.25wt%SnO_x/AC3, the HNO_3-oxidized AC supported catalyst, first in terms of low-temperature CO oxidation in order to find the CO and O_2 dependency of CO oxidation rates, and then to investigate the effect of the presence of H_2 in the feed.

Experimental

Catalyst preparation

Commercial activated carbon NORIT ROX, crushed and sieved to 344-255 μm, was treated with 2 N HCl to remove its ash and accompanying sulfur content, washed with water to remove the HCl, and further oxidized in a 5 N HNO_3 solution followed by rinsing with water. The procedure used for support preparation was previously reported in detail.[7] Sequential impregnation of aqueous tin chloride and hexachloroplatinic

acid solutions was used respectively to prepare 1wt%Pt-0.25wt%SnO_x/AC3 and it was followed by drying overnight at 373K.[8,9]

Reaction experiments

Reaction experiments were conducted in a 4 mm-ID stainless steel fixed-bed down-flow micro-reactor placed inside a 2.4 cm-ID x 50 cm tubular furnace controlled to ±0.5 K by a Shimaden FP-21 programmable temperature controller. Flow rates of research grade gases and gas mixtures were controlled by calibrated Brooks 5850E mass flow controllers. An ATI UNICAM 610 gas chromatograph having a TCD and a concentric column (CTR I) was used for the analysis of reactant and product streams at 303 K under 35 cm^3min^{-1} carrier (He) flow. The catalyst samples used in the reaction experiments were pretreated in situ at 673 K for 2 h with He followed by 2 h of reduction under H_2 flow. Low temperature CO oxidation over the 1wt%Pt-0.25wt%SnO_x/AC3 catalyst was studied in the initial rates region over freshly reduced catalyst samples using the experimental conditions listed in Table 1. Reactant conversions remained essentially constant after 60 min on stream.

Table 1. Experimental conditions of low-temperature CO oxidation and PROX.

Parameters	CO Oxidation	PROX
Temperature, K	383	383
Catalyst, mg	100-150	100
Total flow, cm^3min^{-1}	100-200	150
CO, mol%	1-10	5
O_2, mol%	1-4	2
H_2, mol%	0	5-45
Inert balance	He	He
Time-on-stream, min	90	90

The conversions of CO and O_2 were defined as follows:

$$X_{CO}(\%) = \frac{[CO]_{in} - [CO]_{out}}{[CO]_{in}} x100 \tag{1}$$

$$X_{O_2}(\%) = \frac{[O_2]_{in} - [O_2]_{out}}{[O_2]_{in}} x100 \tag{2}$$

The oxygen in excess with respect to the amount of O_2 required for the oxidation of CO to CO_2 was described by the commonly used process parameter λ:[11]

$$\lambda = \frac{2C_{O_2}}{C_{CO}} = \frac{2P_{O_2}}{P_{CO}} \tag{3}$$

Kinetic measurements were conducted under differential conditions, and intrinsic kinetic data were obtained in the initial rates range. The catalyst mass-based reaction rates, ($-R_{CO}$), were calculated from conversion versus space time ($W_{cat}/F_{CO_{in}}$) data:

$$(-R_{co}) = \frac{x_{CO}}{W/F_{CO_{in}}} \tag{4}$$

where x_{CO} denotes CO conversion, $F_{CO_{in}}$ is the feed CO flow rate measured in $cm^3\ min^{-1}$ and converted to $\mu mol.min^{-1}$, W_{cat} is the catalyst weight in mg, and $(-R_{CO})$ is the reaction rate in $\mu mol.mg^{-1}.min^{-1}$. The space time ($mg.min.\mu mol^{-1}$) was defined as the ratio of mass of catalyst (W_{cat}) to the molar flow rate of CO at the reactor inlet, F_{CO}.

Results and Discussion

Kinetic analysis of low temperature CO oxidation

The 1wt%Pt-0.25wt%SnO_x/AC3 catalyst was evaluated first in terms of its low-temperature CO oxidation behavior in the absence of H_2. Preliminary experiments showed that internal and external mass transfer limitations were negligible. Intrinsic kinetic experiments were conducted at atmospheric pressure and a constant temperature of 383 K using various CO concentrations between 1 and 10 mol% at different O_2/CO molar ratios (λ = 0.67-2.0) and space times (0.14-2.45 mg min μmol^{-1}). In each set of experiments, CO conversion (X_{CO}) data taken at constant feed composition by varying space time (W/F_{CO}) were used to confirm the linear change characteristic of the initial rates region; the data with linear regression constants 98% or better were used in the subsequent individual rate calculations. This is demonstrated for 2 sets of experiments in Figure 1, and representative initial rates of CO oxidation at 383 K are presented in Table 2. O_2 conversions were also measured in all experiments mainly for data control purposes; (X_{CO}) and (X_{O2}) data obtained at various space times and feed compositions were generally consistent within the experimental error, and representative data are presented in Table 3.

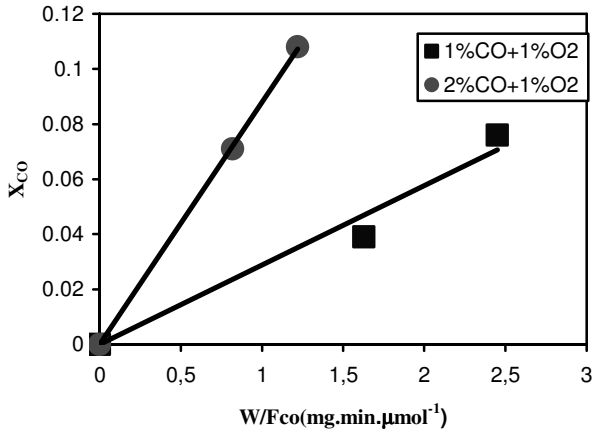

Figure 1. Fractional CO conversion versus space time in CO oxidation at 383 K over 1wt%Pt-0.25wt%SnO_x/AC3 for 2 different feed compositions.

Initial rates of CO consumption were individually extracted from intrinsic kinetic data obtained in 16 experiments run in duplicate under conditions where maximum CO conversions were kept $\leq$ 10%. In the study, 5 different CO and O_2 concentrations corresponding to 4 different λ values were used, and each feed composition was tested at 2-4 different space times. A power-function rate expression was postulated to describe the kinetics of low-temperature CO oxidation at 383 K over 1wt%Pt-0.25wt%SnO_x/AC3:

$$(-R_{CO}) = k\,(P_{CO})^{\alpha}\,(P_{O_2})^{\beta} \tag{5}$$

Table 2. Representative initial rates of low-temperature CO oxidation at 383 K.

P_{CO} (kPa)	P_{O2} (kPa)	λ	Number of duplicated runs	(-R_{CO}) (μmol $h^{-1}mg^{-1}$)	R^2
1.0133	1.0133	2	2	1.801	0.985
2.0265	1.0133	1	2	5.294	0.999
3.0398	1.0133	0.67	2	4.044	0.976
3.0398	1.5199	1	2	4.066	0.998
5.0663	2.0265	0.80	2	6.099	0.993
5.0663	2.5331	1	2	5.526	0.984
10.1325	4.0530	0.80	4	11.538	0.996

Table 3. CO and O_2 conversions at various inlet compositions and space times (T = 383 K; time-on-stream = 90 min).

P_{CO} (kPa)	P_{O2} (kPa)	λ	W/F_{CO} (mg min μmol^{-1})	X_{CO}	X_{O2}
1.0133	1.0133	2	2.45	0.076	0.038
2.0265	1.0133	1	1.22	0.108	0.105
3.0398	1.0133	0.67	0.82	0.053	0.077
3.0398	1.5199	1	0.54	0.039	0.038
5.0663	2.5331	1	0.37	0.033	0.037
10.1325	4.0530	0.80	0.18	0.037	0.046

The parameters (α, β, and k) were evaluated using linearized least squares as well as non-linear regression analysis minimizing the sum of the squared differences of calculated and experimental CO consumption rates:

$$Minimize \left\{ \sum_{i=1}^{n} (R^m_{CO,i} - R^e_{CO,i})^2 \right\} \tag{6}$$

In Eq. (6), "i" is the number of individual experiments that have been duplicated, n= 16, and superscripts "m" and "e" indicate model predicted and experimentally measured values of CO utilization rates, respectively.

Using Eq. (5) and non-linear regression analysis in the MATLAB^{TM} environment, the reaction orders with respect to CO (α) and O_2 (β) are estimated to be 0.96 and -0.31, respectively, indicating that the rate of CO oxidation is directly proportional to the CO partial pressure and is mildly inhibited by the O_2 partial pressure. The apparent reaction rate constant "k" is calculated as 1.78 μmol.mg^{-1}.h^{-1}.$kPa^{-0.65}$. The following rate expression is obtained for CO oxidation over 1wt%Pt-0.25wt%SnO_x/AC3 at 383 K:

$$(-R_{CO}) = 1.78\,(P_{CO})^{0.96}\,(P_{O_2})^{-0.31} \tag{7}$$

The sum of the squared relative differences of calculated and experimental CO consumption rates is determined as 0.0056 (μmol.mg^{-1}.h^{-1})^2. The fit between experimentally measured and model predicted rates is reasonably good with a mean squared error of 0.96; this is demonstrated in Figure 2, which takes into account all individual rates used in the non-linear regression analysis.

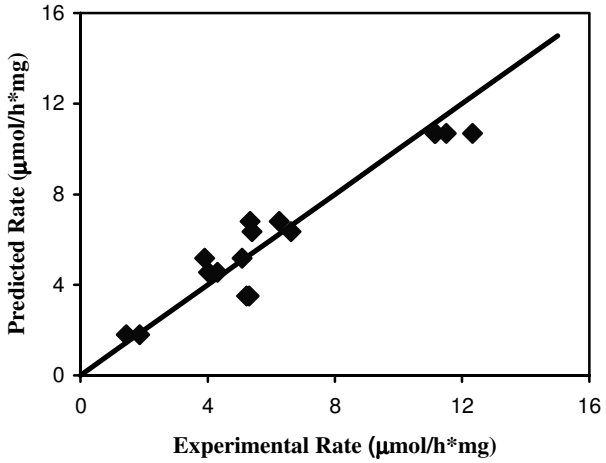

Figure 2. Experimental rates versus calculated rates of low temperature CO oxidation over 1wt%Pt-0.25wt%SnO_x/AC3 under conditions in Table 1.

Studies dealing with CO oxidation over supported Pt catalysts have made a distinction between 2 reaction regimes: a regime where the surface is primarily covered with CO, which is expected to prevail at low temperatures and/or reducing conditions (lower λ values), or a regime in which the surface concentration of CO is rather small, which is likely to occur at higher temperatures and/or oxidizing conditions (higher λ values). The first regime leads to negative reaction orders approaching unity for CO and positive reaction orders for O_2, while the second regime is associated with positive reaction orders close to unity for CO and zero order for O_2.[11] In general, negative orders in CO imply that the Pt surface is effectively saturated by CO whereas positive reaction orders mean that the CO coverage is considerably below saturation under the reaction conditions and, therefore, a decrease in CO partial pressure will also decrease the reaction probability for CO oxidation.[12]

Rate measurements and titration experiments conducted in the 273-353 K interval over Al_2O_3 supported Pt-SnO_2 showed that, at low CO concentrations, CO oxidation was positive first order in CO, which rapidly decreased to zero order as the CO partial pressure was increased.[4] Since oxygen can adsorb on both Pt and SnO_2 sites while CO chemisorbs only on Pt, the drastic change between the 2 regimes was attributed to the shift from an oxygen-covered surface to a CO-covered one. The mechanistic suggestion was that SnO_2 provides suitable sites for dissociative oxygen adsorption, the reaction between adsorbed reactants is instigated by oxygen reverse spill-over from SnO_2 to Pt sites, and, if the transfer of oxygen atoms from SnO_2 to Pt sites is fast enough, the surface reaction can be treated as if it takes place between CO and oxygen adsorbed on Pt sites.

On the other hand, an association at an atomic level occurs upon extensive reduction leading to the formation of PtSn and/or Pt_3Sn alloys which are also proposed as efficient catalysts/sites for CO oxidation.[7,8,13] The Pt-rich Pt_3Sn alloy can adsorb oxygen more readily than Pt or PtSn alloy sites. The activities of AC supported Pt-SnO_x catalysts are strongly influenced by the surface chemistry of the support and the Pt/Sn atomic ratio as well as by catalyst preparation and reduction procedures. Firstly, it must be noted that the HNO_3-oxidized support, AC3, has a high concentration of oxygen-bearing surface groups, mainly carboxylic acid groups, which impart an acidic nature to the support and provide a high concentration of anchoring sites for the metal precursors.[7] During reduction, some of these groups decompose, thus assisting

the formation of Pt_3Sn alloy sites adjacent to Pt sites via a reduction-oxidation cycle. The abundance of anchoring sites on the AC3 surface restricts the mobility of the metallic species by providing many other anchoring sites in close proximity, and the catalyst retains its high metal dispersion. Secondly, sequential impregnation of Sn and Pt precursors, with Sn being introduced first, and reduction with H_2 at 673 K both facilitate the formation of active Pt and Pt-rich alloy sites.[8]

The positive reaction order close to unity (0.96) obtained for CO in the present kinetic study implies that the CO coverage on metallic sites is significantly below saturation while that of oxygen is relatively high as indicated by its mildly negative reaction order of -0.31. Neither the reaction temperature (383 K) nor the λ values (0.67-2.00) used are high enough to bring about this result; therefore, it must be the surface chemistry of the support and the presence of the Pt-rich Pt_3Sn alloy sites close to Pt sites that offer a plausible explanation.

Role of the AC3 support: The AC3 support not only leads to the formation of the Pt_3Sn alloy during catalyst preparation but also enhances the stabilization and transfer of oxygen on the support surface during the reaction; the decomposed oxygen-bearing surface groups leave low-coordination carbon atoms on the AC support, which are ready to interact with oxygen and transfer it to the active metal/alloy sites where the reaction occurs.[7,8] It is likely that rapid oxygen reverse spillover from SnO_x sites onto Pt and Pt_3Sn sites provides a synergistic interaction that also increases the surface coverage of oxygen.

Role of the Pt_3Sn alloy sites: Recent theoretical studies based on quantum mechanical calculations[14,15] have clearly shown that the adsorption strength of CO on Pt_3Sn alloy sites is lower compared to that on Pt sites, which implies enhanced resistance by Pt_3Sn against CO blanket formation/poisoning. The decrease in the overall adsorption strength of CO is caused by (*i*) the decrease in the number of possible adsorption sites, since CO cannot adsorb on Sn-incorporated sites, and *(ii)* the electronic modification of Pt sites by the Sn present in the neighborhood, which results in a reduction of the CO adsorption strength on Pt sites.

It is also known that Sn-containing sites can easily adsorb oxygen; thus, when the Pt_3Sn alloy is present, CO and oxygen adsorption sites are very close to each other, thereby eliminating the difficulties arising from oxygen transfer to Pt sites. The reaction orders with respect to CO and O_2, 0.96 and -0.31, respectively, indicate a reaction taking place on a surface that is mostly covered by adsorbed oxygen with relatively weak CO adsorption.

Effect of H_2 on CO oxidation

CO oxidation and PROX studies previously conducted on 1wt%Pt-0.25wt%SnO_x/AC3 at 423 K in the absence and presence of H_2, CO_2, and H_2O have all shown that its performance is superior, leading to 100% CO conversion under a wide range of feed compositions.[7–10]

In this work, the effect of the presence of H_2 on CO conversions and CO oxidation rates was tested in the initial rates region under conditions in Table 1 by partially replacing the inert He with 5-45 mol% H_2 in a feed containing 5 mol% CO and 2 mol% O_2. Reactant conversions and the selectivity for CO oxidation in H_2-containing feed streams are presented in Table 4. The selectivity for CO oxidation is defined as the amount of oxygen consumed in CO oxidation divided by the total amount of oxygen consumed, taking into consideration the λ value and the reaction stoichiometry.

The addition of H_2 into the feed increases both CO and O_2 conversions. When the amount of H_2 in the feed is low and equal to CO, namely 5 mol%, CO conversion is more than doubled, increasing from 2.9%

in the absence of H_2 to 7.1% in its presence, and the selectivity obtained for CO oxidation is remarkably high, 70%. CO and O_2 conversions remain almost constant as the H_2 in the feed is increased up to ca. 15 mol% (Figures 3 and 4); the selectivity for CO oxidation stays around 70%-75%. When the H_2 content is further increased from 17.5 to 30 mol%, however, CO conversion also increases from 15% up to 28%-29%, which is accompanied by a rapid increase in O_2 conversion from 26% to 78%-79% in the same interval at a space time as low as 0.33 mg min μmol^{-1}. Both conversions level out at 30 mol% H_2 and stay in the same range even when 45 mol% H_2 is introduced into the feed stream. The selectivity for CO oxidation rapidly declines from 75% at 17.5 mol% H_2 to 46% at H_2 concentrations of 30 mol% and above.

Table 4. CO and O_2 conversions in H_2-containing feed streams and selectivity for CO oxidation ($\lambda = 0.80$; T = 383 K; W_{cat}/F_{CO} = 0.33 mg min μmol^{-1}; time-on-stream = 90 min).

CO mol%	O_2 mol%	H_2 mol%	X_{CO}	X_{O2}	S_{CO} (%)
5	2	5	0.071	0.126	70
5	2	10	0.065	0.123	66
5	2	17.5	0.156	0.260	75
5	2	20	0.177	0.399	56
5	2	30	0.290	0.784	46
5	2	45	0.281	0.769	46

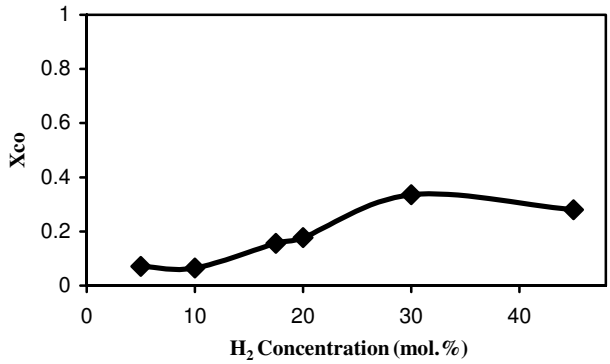

Figure 3. Effect of H_2 concentration on CO conversion in PROX at 383 K (5 mol% CO, 2 mol% O_2 and balance He).

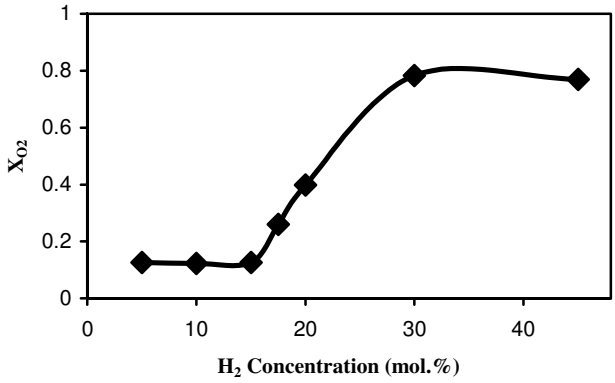

Figure 4. Effect of H_2 concentration on O_2 conversion in PROX at 383 K (5 mol% CO, 2 mol% O_2 and balance He).

It is assumed that the addition of hydrogen to a feed containing CO and O_2 does not essentially change the mechanism of CO oxidation over the catalyst. In fact, in situ DRIFTS measurements on a γ-Al_2O_3 supported Pt catalyst with feed containing 75% H_2 showed that the surface coverage of CO still corresponded to its saturation value at the reaction temperature;[12] this was later confirmed by PROX studies conducted over carbon supported bimetallic PtSn catalysts.[16] The H_2-induced increase observed in the CO oxidation rate was attributed to the interaction between the hydroxylated Al_2O_3 support and the CO adsorbed on Pt sites,[11] which implies that the effect of H_2 on CO oxidation rate depends on the nature of the support material. In the present work, the enhancement in the CO oxidation rate over 1wt%Pt-0.25wt%SnO_x/AC3 with the addition of H_2 is almost 10-fold at H_2 concentrations $\geq$ 30 mol%, which are typical of the H_2 concentrations existing in the inlet stream of the PROX reactor located in a fuel processor. A possible explanation may be that the interaction of H_2 with oxygen-bearing surface groups, and/or with oxygen species adsorbed on Pt and Pt_3Sn sites, diminishes the oxidizing conditions provided by the AC3 support and releases some of the active metallic sites for CO adsorption which, in turn, leads to the H_2-induced enhancement observed in the CO oxidation rates. There are reports[17,18] showing that OH groups are involved in oxidizing the CO present in H_2-rich streams over Rh catalysts. Additional theoretical and experimental work is necessary in order to discuss the role of OH groups on PROX over bimetallic Pt-Sn catalysts.

Conclusion

The kinetics of low temperature CO oxidation on 1wt%Pt-0.25wt%SnO_x/AC3 was investigated at 383 K over a relatively wide range of CO (1-10 mol%) and O_2 (1-4 mol%) concentrations corresponding to λ values of 0.67-2.0. A power function rate expression with positive dependence on carbon monoxide (0.96) and negative dependence on oxygen (–0.31) is proposed for low temperature CO oxidation in the absence of H_2, indicating that the reaction takes place on a surface that is predominantly covered by adsorbed oxygen with relatively weak CO adsorption. The easy oxygen transfer provided by the AC3 support as well as the Pt-rich alloy sites with high oxygen adsorption capacity may be responsible for the reaction orders observed. The enhancement in the CO oxidation rates over 1wt%Pt-0.25wt%SnO_x/AC3 with the addition of H_2 into the feed is almost 10-fold at H_2 concentrations above 30 mol% where the CO oxidation selectivity is 46%.

Acknowledgement

Financial support was provided by the TÜBİTAK project 104M163 and Boğaziçi University projects BAP-06HA501 and DPT-03K120250. The TÜBA-GEBIP grant to A. E. Aksoylu is also acknowledged.

References

1. D.L. Trimm and Z.İ. Önsan, **Catal. Rev. Sci. Eng. 43**, 31-84 (2001).
2. D.L. Trimm, **Appl. Catal. A Gen. 296**, 1-11 (2005).
3. R.J. Farrauto and C.H. Bartholomew, **"Fundamentals of Industrial Catalytic Processes"**, Blackie Academic and Professional, London, p. 654, 1999.

4. K. Grass and H.G. Lintz, **J. Catal. 172**, 446-52 (1997).
5. A.N. Akın, G. Kılaz, A.İ. İşli and Z.İ. Önsan, **Chem. Eng. Sci. 56**, 881-88 (2001).
6. A. Boulahouache, G. Kons, H.G. Lintz and P. Schulz, **Appl. Catal. A: Gen. 91**, 115-23 (1992).
7. A.E. Aksoylu, M.M.A. Freitas and J.L. Figueiredo, **Appl. Catal. A Gen. 192**, 29-42 (2000).
8. A.E. Aksoylu, M.M.A. Freitas and J.L. Figueiredo, **Catal. Today 62**, 337-46 (2000).
9. Ş. Özkara and A.E. Aksoylu, **Appl. Catal. A Gen**. **251**, 75-83 (2003).
10. E. Şimşek, Ş. Özkara, A.E. Aksoylu and Z.İ. Önsan, **Appl. Catal. A: Gen. 316**, 169-74 (2007).
11. M.J. Kahlich, H.A. Gasteiger and R.J. Behm, **J. Catal.**. **171**, 93-105 (1997).
12. M.M. Schubert, M.J. Kahlich, H.A. Gasteiger and R.J. Behm, **J. Power Sources 84**, 175-82 (1999).
13. J. Arana, P. Ramirez de la Piscina, J. Llorca, J. Sales, N. Homs and J.-L.G. Fierro, **Chem. Mater. 10**, 1333-42 (1998).
14. M.A. Gülmen, A. Sümer and A.E. Aksoylu, **Surface Science 600**, 4909-21 (2006).
15. A. Sümer, M.A. Gülmen and A.E. Aksoylu, **Surface Science 600**, 2026-39 (2006).
16. M.M. Schubert, M.J. Kahlich, G. Feldmeyer, M. Hüttner, S. Hackenberg, H.A. Gasteiger and R.J. Behm, **Phys. Chem. Chem. Phys. 3**, 1123-31 (2001).
17. A.B. Mhadeshwar and D.G. Vlachos, **J. Phys. Chem. B**, **108**, 15246-58 (2004).
18. A.B. Mhadeshwar and D.G. Vlachos, **J. Catal. 234**, 48-63 (2005).